Conformation and Fracture of Polystyrene Chains in Extensional Flow Studied by Numerical Simulation

ARTICLE *in* MACROMOLECULES · MAY 1996

Impact Factor: 5.8 · DOI: 10.1021/ma9513980

3 AUTHORS:

Kenneth D Knudsen
Institute for Energy Technology
116 PUBLICATIONS **1,287** CITATIONS
SEE PROFILE

J. G. Hernández Cifre
University of Murcia
47 PUBLICATIONS **473** CITATIONS
SEE PROFILE

José García de la Torre
University of Murcia
217 PUBLICATIONS **6,114** CITATIONS
SEE PROFILE

Conformation and Fracture of Polystyrene Chains in Extensional Flow Studied by Numerical Simulation

K. D. Knudsen, J. G. Hernández Cifre, and J. García de la Torre*

Departamento de Química Física, Facultad de Química, Universidad de Murcia, 30071 Murcia, Spain

Received September 18, 1995; Revised Manuscript Received February 9, 1996[⊗]

ABSTRACT: We have studied the behavior of flexible polymer chains as they pass from a large diameter tube into a narrow capillary using the Brownian dynamics simulation technique. The polymer/solvent system studied was a very dilute solution of polystyrene in cyclohexane at a temperature of 35 °C. The polymer was modeled as a bead−spring chain, parameterized as to reproduce real polymer/solvent conditions. The end-to-end distance and the radius of gyration were seen to change abruptly as the chain entered the orifice of the capillary, giving rise to fracture of the polymer. In addition to chain fracture in the capillary orifice, chains were also observed to fracture within the capillary, and the fracture yield did not stabilize until a distance of about 0.3 cm into the capillary for an orifice diameter of 0.04 cm and the other instrumental dimensions and flow rates used in the study. We found that when the hydrodynamic interaction effect (HI) was not taken into consideration, the critical flow rate for fracture at the orifice showed a dependence on the molecular weight as $Q_{crit} \sim M^{-1.8}$. This exponent is close to the theoretical value for breakage of fully extended chains. When HI was accounted for, the exponent was found to be significantly lower (−0.95), indicating chain fracture in a less extended conformation and showing that hydrodynamic interaction should not be disregarded in studies of polymer fracture in transient extensional flow.

Introduction

Long-chain polymers in solution have a variety of technical applications, and in most real flow systems the polymers encounter flow with a predominant extensional character. This may be flow through constrictions in pipes, porous media, or filters, as well as in laboratory devices such as pipets and narrow orifices. In extensional flows the polymer chains may fracture if the flow rate is sufficiently high. Such degradation is often an undesirable effect. If chain rupture occurs during the technological processing of solutions or melts, it will alter the flow behavior and thus the processing characteristics and eventually affect the final products. Apart from the technological aspects, the fracture process is also of scientific interest since it provides an opportunity to observe the effects of extreme forces acting on the polymer chain.

During the last 15 years, a substantial amount of experimental data has been gathered on polymers in extensional flow, examples are the works of Odell, Keller, and co-workers,[1−3] Nguyen and Kausch,[4,5] and Fuller and co-workers.[6,7] However, few theoretical predictions exist for the behavior of the polymer chains in this type of flow. This is especially the case for so-called transient extensional flows, where the residence time of the polymer chain may be comparable to or even shorter than its relaxation time, leading to experimental results quite distinct from those obtained in situations with steady state flow.

However, use of computers to simulate the Brownian dynamics of model polymer chains has recently evolved as an alternative way of studying these processes. Some studies have already been undertaken and demonstrated the ability of this method in reproducing experimental data while probing both conformation and fracture in extensional flow. Fracture distribution has been studied in convergent flow by Reese and Zimm[8] for a model of DNA, and López Cascales and García de la Torre have studied steady state properties and fracture kinetics in elongational flow of uniaxial type.[9,10]

We have recently[11] performed, by means of numerical simulation, a preliminary exploration of the fracture process of a model of polystyrene chains in cyclohexane while subjected to sink (convergent) flow in a tube/capillary system. In the present study we go more into detail concerning the behavior of the molecules in the flow, studying the radius of gyration, end-to-end distance, and length of specific chain segments, as well as the dependence of the molecular weight of the polymer on the critical flow rate for fracture. We also wanted in this work to include the effect of hydrodynamic interaction (HI) between different parts of the chain, studying what influence HI may have on fracture yield and scaling exponents for critical flow rate vs molecular weight. The hydrodynamic interaction effect has been difficult to include in theoretical solutions of the behavior of polymers in extensional flow.

Model and Simulation Method

The polymer/solvent system studied in the present work was a very dilute Θ-solution of monodisperse polystyrene in cyclohexane at 35 °C. The polymer molecule is modeled as a bead−spring Rouse chain with Hookean springs. The spring constant H then equals $3kT/b^2$, where the parameter b is the root-mean-square spring length. The instantaneous spring length is denoted q. To parameterize the model, we have chosen the molecular weight per bead, M_1, to be 1×10^5. The number of beads, $N = M/M_1$, required for a polymer of around 1 million in molecular weight is then not prohibitively high for the computer simulation. A polymer with molecular weight 2×10^6 will with this assumption be modeled as a 20-bead chain. Anyhow, it can be shown that the final results will not depend on the choice of M_1 provided that N is large enough. By combining the experimentally obtained expression (in Θ-solution and at equilibrium) for the relation between the radius of gyration of a flexible polymer and its molecular weight, $\langle S^2 \rangle = C_s M$, with the theoretical expression for $\langle S^2 \rangle$ for a Rouse chain,[12] $\langle S^2 \rangle = b^2(N^2 - 1)/6N \approx b^2N/6$, we obtain an expression for the root-mean-square spring length, $b^2 = 6C_sM_1$. Employing now the experimentally found value[13,14] for polystyrene in cyclohexane at 35 °C, $C_s = 7.9 \times 10^{-18}$ cm^2 mol/g, we finally end up with a value of 21.7 nm for b.

* To whom correspondence should be addressed.

[⊗] Abstract published in *Advance ACS Abstracts,* April 1, 1996.

S0024-9297(95)01398-2 CCC: $12.00

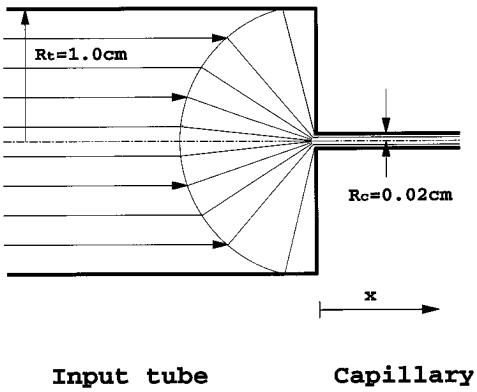

Figure 1. Schematic drawing of the simulated system. In the cylindrical tube we assume Poiseuille flow and near the orifice convergent flow (starting at a distance R_t from the orifice).

We adopt the limiting stretching energy model proposed by Lopez Cascales and Garcia de la Torre.[9] In this model, the springs are considered to break when the stretching energy reaches some limiting value, A (the spring dissociation energy), corresponding to a spring length of $q_{max} = (2A/H)^{1/2}$. The simulation results, such as the critical flow rate, will depend quantitatively on the value of A. However, the general conclusions and scaling exponents will not be influenced by this choice. For the present simulations the value has been A = 30 kcal/mol.

The simulated system is the same as that described in our previous study.[11] A schematic of the setup is shown in Figure 1. The sample is contained in a cylindrical tube of radius R_t = 1.0 cm which has at its end a narrow constriction, so that the fluid passes through a small orifice of radius R_c = 0.02 cm. The orifice is followed by a thin capillary, so that the whole device has a syringe-like character. The volumetric flow rate through the device is denoted Q. In the cylinder we have laminar Poiseuille flow, and the relation between the flow rate and the velocity along the center line is given by the expression: $Q = (\pi R_t^2/2)v_c$. When the fluid approaches the orifice, at a distance of R_t the stream lines converge and we assume to have sink (convergent) flow. In the sink flow region, the velocity along a stream line depends on the distance to the orifice, ρ, as $v = v_o\rho_o^2/\rho^2$. Here $\rho_o = R_t$, and v_o is the velocity in that stream line at the end of the Poiseuille region, determined by the instrumental dimensions and the flow rate. Thus the velocity increases inversely proportional to the second power of the distance from the orifice. At the entrance of the orifice the sink flow is considered to terminate, and from this point on the flow is considered laminar. The position where the flow pattern changes is situated at a distance R_c (equal to the capillary radius) from the origin of coordinates for the sink flow.

The extensional rate is given by the expression $|dv(\rho)/d\rho|$ and equals, in the region of convergent flow, $\dot{\epsilon} = 2v_o\rho_o^2/\rho^3$. In Figure 2 we have illustrated the extensional rate profile vs position relative to the apex of the orifice (negative x-values correspond to positions in front of the orifice). We can see that the maximum value of $\dot{\epsilon}$ with this flow rate (Q = 1cm^3/s) will be ca. 1.4×10^5 s^{-1}. Changing the value of Q will change the maximum $\dot{\epsilon}$-value accordingly. The peak in $\dot{\epsilon}$ occurs at an x-value slightly negative because the origin of coordinates was chosen to be at the apex of the input cone of the flow field, which is situated slightly inside the geometrical start of the capillary. The variation of $\dot{\epsilon}$ with position is qualitatively very similar to that found in the real device of Nguyen and Kausch (see Figure 4.a in ref 5), with a strong but progressive increase in $\dot{\epsilon}$ as the orifice is approached and a more sudden decrease past the maximum. Thus our mathematically simplified flow field can be a good representation of the real one.

In the simulations, the polymer chain was initially placed with its center of mass on the center line of the device, in a random conformation and at a distance to the orifice equal to the distance traveled by the chain during a period equal to 3 times the first Rouse relaxation time of the molecule. This relaxation time was calculated from $\tau_1 = (\zeta/2H)/[4 \sin^2(\pi/2N)]$.

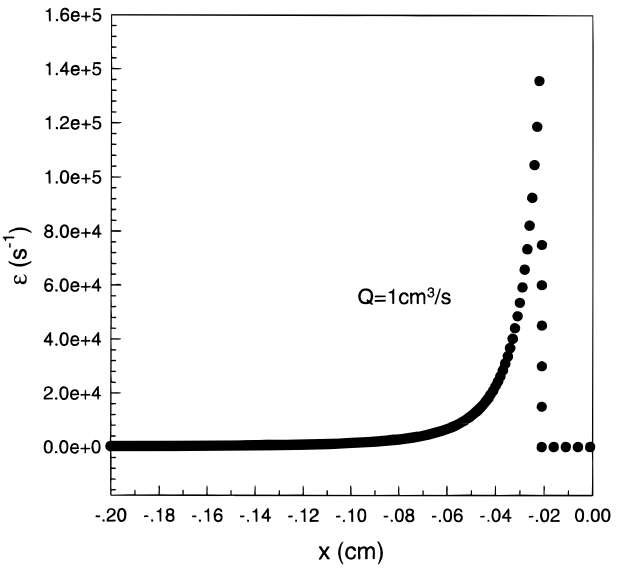

Figure 2. Profile of the extensional flow rate ($\dot{\epsilon}$) in front of the capillary orifice. The plot is made with volumetric flow rate (Q) equal to 1 cm^3/s.

Here ζ is the friction coefficient of a bead in the polymer chain, $\zeta = 6\pi\eta_s\sigma$, where η_s is the solvent viscosity and σ the bead radius.[12] We want the distance to be reasonably short to avoid very time consuming simulations. However, in our previous study,[11] we found that a distance of 2−3 times the distance traveled during τ_1 was necessary to ensure that the results did not depend on the initial distance. This is of relevance when comparing our results with data obtained in laboratory experiments. When we include hydrodynamic interaction in our simulations, we still use the Rouse relaxation time mentioned above (HI not included) to decide upon the initial distance, thereby making a conservative choice since the relaxation time with HI is less than without HI.

For simulating the evolution of the polymer chains as they flow through this device, we employed the Brownian dynamics algorithm of Ermak and McCammon[15] with the predictor-corrector improvement of Iniesta and Garcia de la Torre.[16] In this study we present mainly results without HI because the calculations with HI are much more time consuming. We included HI only where this effect was expected to have some quantitave influence, as in the scaling exponent for fracture vs molecular weight. For the calculations with HI, we employ the Rotne−Prager−Yamakawa tensor.[17]

Using the above-mentioned procedure, Brownian trajectories in space were generated for a sample containing a sufficiently large number of chains. The time step, Δt, was equal to 30 ns. This value is much smaller than the primary relaxation time of the polymer, a necessary requirement of the simulation procedure to work correctly. The calculations were carried out in a SG Indigo workstation with a 4400 processor. The CPU time is obviously proportional to the number of chains and simulation steps. We worked with samples of about 10^3−10^4 chains, with a number of steps of the order of 10^4−10^5 steps/chain. The particular conditions of each case depended on the chain length, N, and the flow rate, Q. For N = 20 beads, one chain trajectory of 10^5 steps took 154 CPU s in the no-HI case and 1060 s with HI.

Dimensionless quantities were used throughout the simulations. Lengths are divided by b (the root-mean-square spring length), forces by kT/b, and times by $\zeta b^2/kT$. Other dimensionless quantities follow from these definitions.

In the simulations the polymer was initially placed on the center line of the device at a distance sufficiently far from the orifice, as explained earlier. Brownian trajectories were then simulated for ensembles containing on the order of 1000 molecules. While following the trajectory of one molecule, the values of radius of gyration, end-to-end distance, and segment length were stored at equally spaced time intervals to later obtain the evolution profile for these parameters. We also monitored every spring for fracture ($q > q_{max}$) at each step in

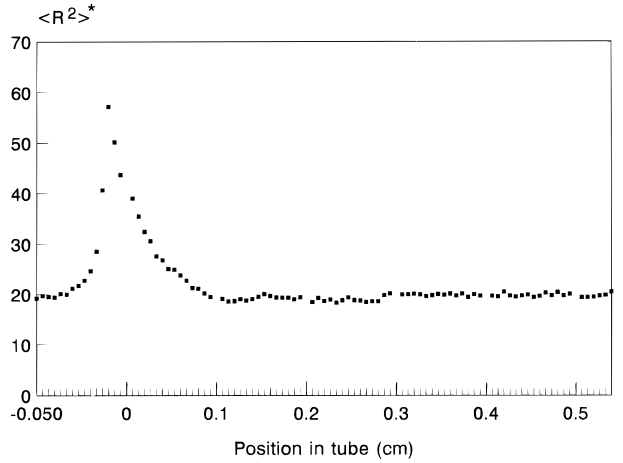

Figure 3. Evolution of the mean-square end-to-end distance in dimensionless form ($\langle r^2\rangle^* = \langle r^2\rangle/b^2$, with $b = 21.7$ nm; see text) of the polystyrene chains as they move into the capillary orifice and down the capillary. The average was performed over 1000 chains. The volumetric flow rate (Q) was equal to 0.3 cm^3/s. The capillary orifice corresponds to "position in tube" equal to zero. The molecular weight of the polymer chain model was 2×10^6.

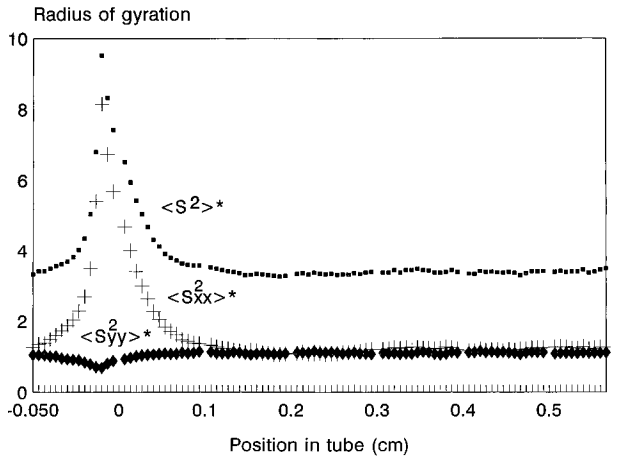

Figure 4. Evolution of the mean-square radius of gyration in dimensionless form ($\langle S^2\rangle^* = \langle S^2\rangle/b^2$) of the polystyrene chains, together with the averaged components $\langle S_{xx}{}^2\rangle^*$ and $\langle S_{yy}{}^2\rangle^*$ of the radius of gyration tensor, as the chains move into the capillary orifice and down the capillary. The average was made over 1000 chains. The volumetric flow rate (Q) was equal to 0.3 cm^3/s. The molecular weight of the polymer chain model was 2×10^6.

the simulation, registering the molecular weight of the resulting two molecular fragments. Carrying out this for all the chains in the sample allowed the molecular weight distribution to be evaluated. In this study we monitored what happened to the molecules in the orifice and at different positions in the capillary, but we did not consider capillary end effects in the context of what may occur when the molecules leave the capillary on its right end side. The initial molecular weight of the polymer was 2×10^6 in most of the work, except for the studies we made about the dependence of critical flow rate upon molecular weight, where we employed molecular weights between 5×10^5 and 2×10^6.

Results and Discussion

In our setup, the extensional rate is very dependent on distance from the orifice, as shown in Figure 2. One would therefore expect that the mean-square end-to-end distance ($\langle R^2\rangle$) and the mean-square radius of gyration ($\langle S^2\rangle$) of the polymer chains also would show a behavior drastically dependent on the position of the chain in the tube system.

In Figure 3 we have plotted the average square end-to-end distance (in dimensionless form) for an ensemble of 1000 chains ($M = 2 \times 10^6$) as function of position in the simulated tube system. Position $x = 0$ corresponds to the apex of the orifice (see Figure 1), and the chains were followed up to a distance of about 0.5 cm into the thin part of the tube (capillary). At their initial position in front of the orifice, the chains start with a random conformation, a fact that is confirmed by the value of ca. 20 for $\langle R^2\rangle^*$ at the left end of the curve (for a random coil, we have theoretically that $\langle R^2\rangle = (N - 1)b^2$, which is equal to $19b^2$ for a chain consisting of 20 beads). Just in front of the orifice the end-to-end distance is seen to increase abruptly, which is consistent with the observation[8,11] that chains may fracture while entering into the capillary. We see from the sharp form of the $\langle R^2\rangle$ curve that the fracture is most likely to occur very close to the orifice, even though the chain may have started its journey far upstream from the capillary. The flow rate used for the data in Figure 3 was kept fairly low ($Q =$ 0.3 cm^3/s), in order to avoid chain fracture and thus get representative results for $\langle R^2\rangle$.

The average square radius of gyration for an ensemble of 1000 chains while traveling down the tube is shown in Figure 4. As one would expect, $\langle S^2\rangle$ shows a behavior qualitatively similar to that of $\langle R^2\rangle$, with a maximum relative increase at this flow rate of ca. 3. As is the case for $\langle R^2\rangle$, $\langle S^2\rangle$ is seen to start decaying in the orifice at the transition point between sink flow and laminar Poiseuille flow. In the setup used, the extensional flow rate falls directly to zero here (see Figure 2), since we have neglected the small transition zone between the two types of flow that will exist in practice. The values of $\langle R^2\rangle$ and $\langle S^2\rangle$ can of course not change in the same manner as $\dot{\epsilon}$, since they are expected to experience a change governed principally by the primary relaxation time of the molecules. Looking at the decay of $\langle S^2\rangle$ in Figure 4, $\langle S^2\rangle$ has been reduced with a factor of $1/e$ when the chain has traveled about 0.06 cm into the capillary after cessation of the extensional flow. This corresponds to a decay time of ca. 125 μs (the flow rate was $Q = 0.3$ cm^3/s), which is slightly above the first relaxation time of the Rouse model of the molecule ($\tau_1 = 73$ μs), illustrating the point mentioned above that the change back to near-equilibrium values in $\langle R^2\rangle$ and $\langle S^2\rangle$ seems to be governed principally by τ_1.

In Figure 4 are also shown the averages $\langle S^2{}_{xx}\rangle^*$ and $\langle S^2{}_{yy}\rangle^*$ of the radius of gyration tensor. The first parameter tells us about the average extension in the x-direction, which is the direction of flow in our setup. From the nature of the extensional flow field, one expects that the polymer chains will experience forces that tend to align and stretch out the chains along the flow direction, and this corresponds well with the results obtained for $\langle S^2{}_{xx}\rangle$. On the other hand, $\langle S^2{}_{yy}\rangle$ shows a dip at the point where $\langle S^2{}_{xx}\rangle$ has its maximum, illustrating that the extension in x-direction goes together with a compression in the plane normal to the direction of flow. However, the relative change in size in this direction is much smaller than the increase in chain dimensions in the x-direction, which is why one can observe experimentally a drastic increase in solution viscosity (η) when polymer chains are subjected to flow fields of elongational type.[18,19]

We have also studied the variation in the average length of the middle segment (spring no. 10 in a 20-bead chain) and the end segment in the chain as the chain passes along the tube system. These parameters are illustrated in Figure 5 (in dimensionless units). It can be seen that, while entering the orifice, the exten-

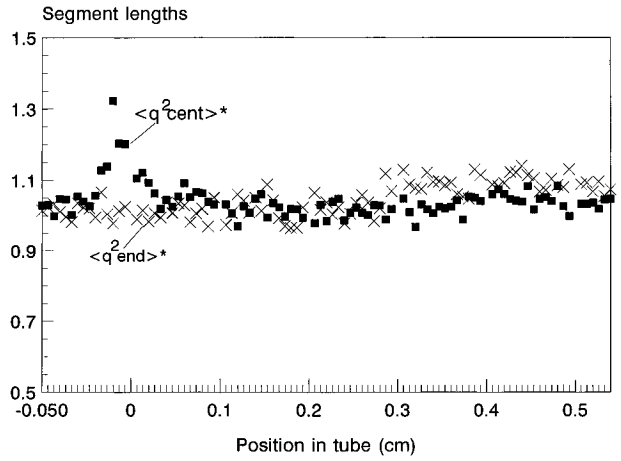

Figure 5. Evolution of the mean-square segment lengths in dimensionless form ($\langle q^2\rangle^* = \langle q^2\rangle/b^2$) of the polymer chains as they move into the capillary orifice and down the capillary. The symbol q_{cent} represents the length of the central segment, and the symbol q_{end} represents the length of the end segment. The average was made over 1000 chains. The volumetric flow rate (Q) was equal to 0.3 cm^3/s. The molecular weight of the polymer chain model was 2×10^6.

sion of the end segment is insignificant compared to that of the central segment in the chain. This is explicable by looking at the solution of the Langevin equation for the separation between two points on the chain,[20] which shows that in elongational flow the tension will be higher in the chain center than near the ends of the chain.

In Figure 6A is shown a snapshot of one molecule in its initial conformation, that is, before the flow field has had any effect on the molecule. The chain is in a random coil conformation, which was produced by selecting the direction of each bead connector vector by means of a random number generator. Figure 6B shows the same molecule just before it enters the orifice, and we can see that the chain has been considerably extended (in the direction of flow), with the major extensions in the segments situated around the central part of the chain.

We now move from the study of conformational properties over to looking at the fracture of the polystyrene chains. When studying the fracture process, we noticed not only that chains broke in the orifice of the capillary but that fracture occurred also well inside the capillary. In Figure 7 we have plotted the total fracture (in percent of total number of chains used in the simulation) monitored at various distances into the capillary for two different flow rates, $Q = 3$ and 10 cm^3/s, respectively. (We have here used Q-values high enough to get significant fracture.) We can see that the fracture yield increases slowly from the orifice and into the capillary and does not reach a maximum until around 0.3−0.5 cm into the capillary. Our interpretation of this observation is that for the chains that did not break at the moment of entering the capillary orifice, while the molecules later tumble down the capillary, the energy that the chains took up during the abrupt extension may later distribute itself more or less randomly along the molecule and accumulate into one of the chain bonds, being sufficiently high to break the bond. In Figure 7 we have also plotted the residence time of the molecule, that is, the time spent in traveling down the capillary as function of distance from the orifice. We can see that when the fracture yield has reached its maximum, the residence time is roughly one-half to two-thirds of the first relaxation time of the chain ($\tau_1 = 73\ \mu$s, also marked in the figures), suggesting the possibility that for the fracture that occurs within the capillary, the primary relaxation time may be used to find an upper limit for the distance up to which fracture may take place. We recall here that, for simplicity, in our simulation all the molecules move along the center line, at which $\dot{\epsilon}$ is, for a given distance to the orifice, slightly above the average for that distance. This may have some influence in the individual, numerical results, but it must not affect the overall trends, the qualitative aspects, and the scaling exponents.

In Figure 8A, we have used a population of a large number of chains (10 000) to make a histogram of the distribution of chain fragments in the orifice of the capillary. The initial molecular weight was 2×10^6, and only the chains that experienced fracture are included in the figure. The distribution is seen to have a bell-like shape, centered around 1×10^6, indicating that the majority of the chains were fractured around the central part of the chain. This result is similar to that obtained by Reese and Zimm[8] in their studies of DNA fracture. In Figure 8B is shown the distribution obtained at a point well within the capillary (where the fracture yield has reached its maximum). To obtain this histogram we have subtracted the fracture that took place in the orifice from the total fracture found at a point inside the capillary. In this case we observe a distribution that is much more uniform, indicating that the fracture that occurs within the capillary takes place more randomly along the polymer chain, a fact that supports our interpretation about the chain fracture process within the capillary given in the preceding paragraph.

Theory predicts[21] that when the polymer chains break in the fully stretched out state, the relation between critical flow rate and molecular weight will have an exponent equal to −2.0 ($Q_{crit} \sim M^{-2.0}$). This result has also been observed experimentally[21,22] in stagnant elon-

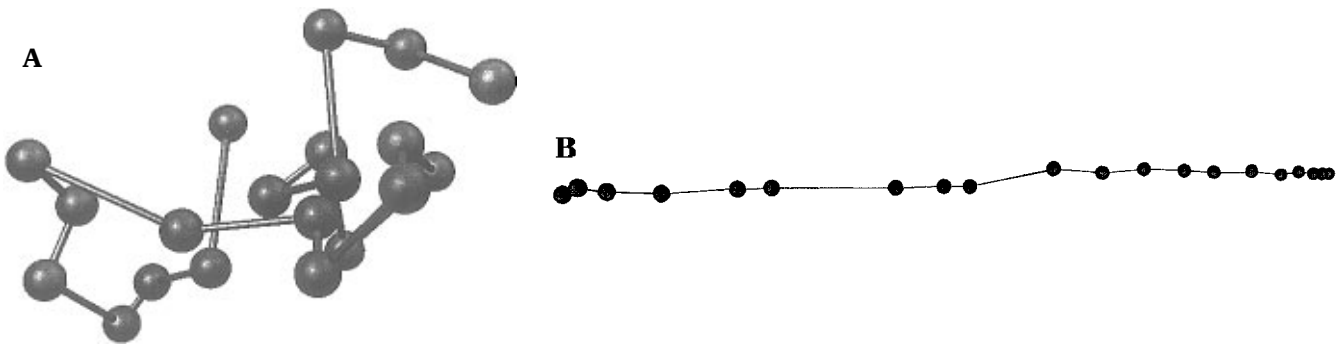

Figure 6. Snapshot of one macromolecular chain at different positions of its travel through the simulated system: (A) initial conformation and (B) chain in extended form while entering the capillary orifice. Volumetric flow rate (Q) equal to 3 cm^3/s. The molecular weight of the polystyrene chain model was 2×10^6.

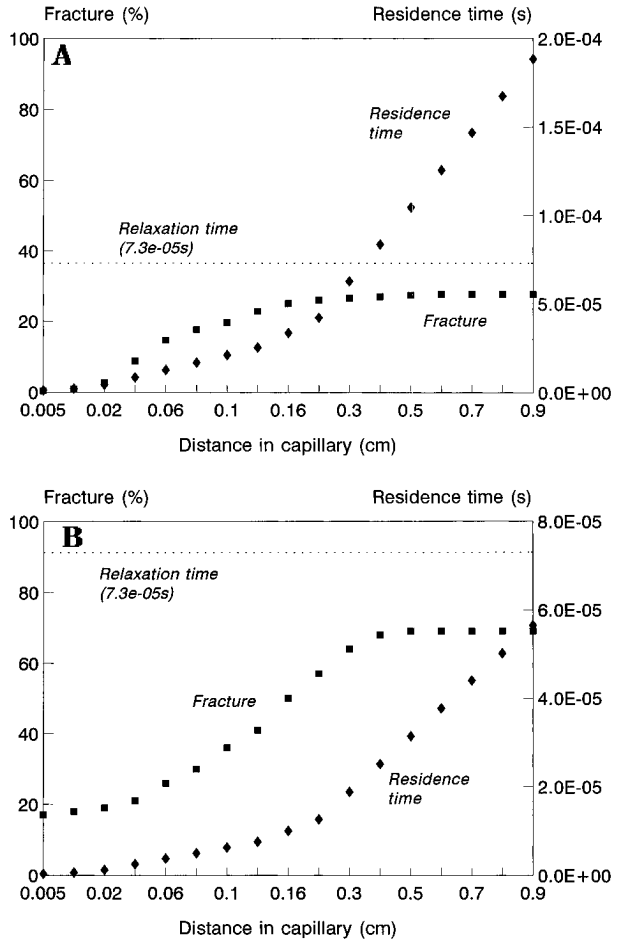

Figure 7. Fracture yield in percentage of initial number of chains (left axis) as function of distance traveled into the capillary for polystyrene chains with molecular weight 2×10^6. The residence time for the chain in the capillary is also shown (right axis): (A) volumetric flow rate (Q) equal to 3 cm^3/s and (B) $Q = 10$ cm^3/s; 500 chains were used in the study.

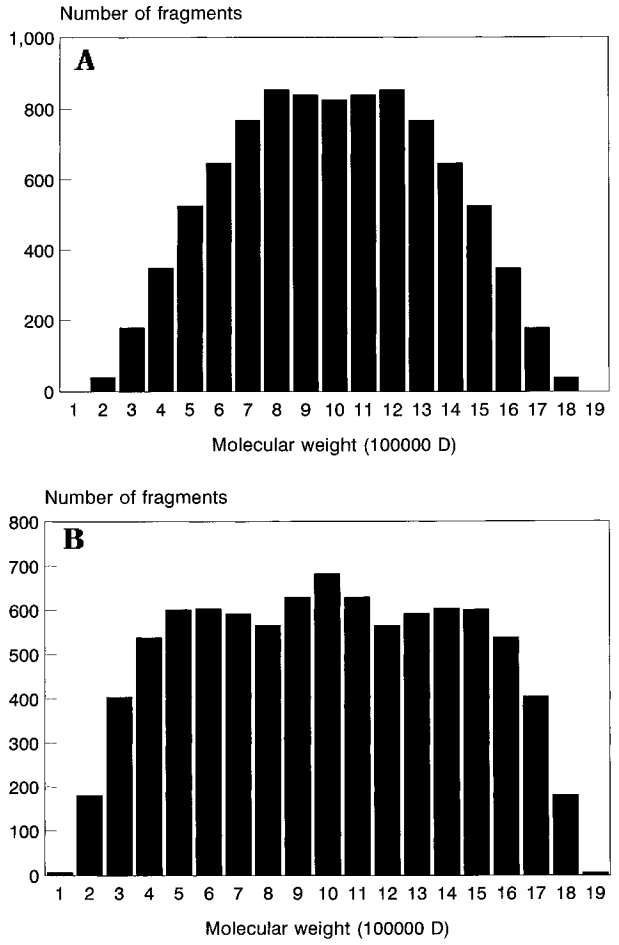

Figure 8. Distribution of molecular weight of the fracture fragments of polystyrene ($M = 2 \times 10^6$) at the capillary orifice (A) and 0.9 cm into the capillary (B). Volumetric flow rate (Q) = 25 cm^3/s. The population consisted of 10 000 polymer chains.

gational flow. For the transient flow studied in the present work, we have made a study of fracture in the capillary orifice for different molecular weights, obtaining results as shown in Figure 9A. The aspect of these simulation results is very similar to that of the results of Nguyen and Kausch in their experimental transient flow (see Figure 6 in ref 4). From plots like Figure 9A, we obtain the observed critical flow rate for fracture for each molecular weight (extracted by means of a second-order regression through the data points). Actually, the values in Figure 9A correspond to simulations without HI, which, as commented above, was the case most easily studied because of its low computational cost. Plotting the Q_{crit} values so observed vs molecular weight (Figure 9B), we get a negative slope of value -1.8 ± 0.2 for the no-HI case. Thus, the chains break much easier as the molecular weight is increased, and the exponent is close to the theoretical value for fracture in the fully extended state (leading to midchain fracture). This result corresponds well with the fragment distribution in Figure 8A, which shows a preference for scission near the center of the chain.

Although very time consuming, we also made some simulations where we included HI between the different parts of the chain. The data about fracture in the orifice for different molecular weights when HI was included (Figure 10A) showed a weaker dependence on the molecular weight than without HI. We obtained an exponent equal to -0.95 ± 0.2, showing that when HI was considered the chains were broken in a less stretched out conformation. Figure 10B is a histogram of the fragment distribution after fracture. This histogram is similar to that of Figure 8A (no-HI), although slightly more extended against lower and higher molecular weights. It has been shown before[23] that one effect of HI is to reduce the overall dimensions of the chain in flow. The reason for the clear difference in molecular weight dependence observed in the two cases (with and without HI) may therefore be that the hydrodynamic interaction tends to protect the central part of the molecule from accumulating the highest stress and that the possibility of reaching a stress high enough for fracture is then more equally distributed along the molecule. The histogram of Figure 10B also seems to support this, since we observe a dip at the molecular weight corresponding to breakage at the chain center. However, we can not be completely sure that this dip is not some unforeseen artifact of the simulation procedure. We think that our results from simulations where HI was included are closer to the real experimental situation, and in experiments with a transient extensional flow device, although only partly similar to the one we have modeled in our simulations, exponents of -0.95 and -1.3 were obtained in the relationship between molecular weight and critical flow rate.[4,5] Besides, Rabin has argued from a theoretical point of view[24,25] that the exponent should be close to -1.0 in transient flow. This author obtained an exponent equal to -2ν, ν taking values from 0.5 (Θ-solution) to 0.6 (good solvent). If we apply for ν the value 0.5,

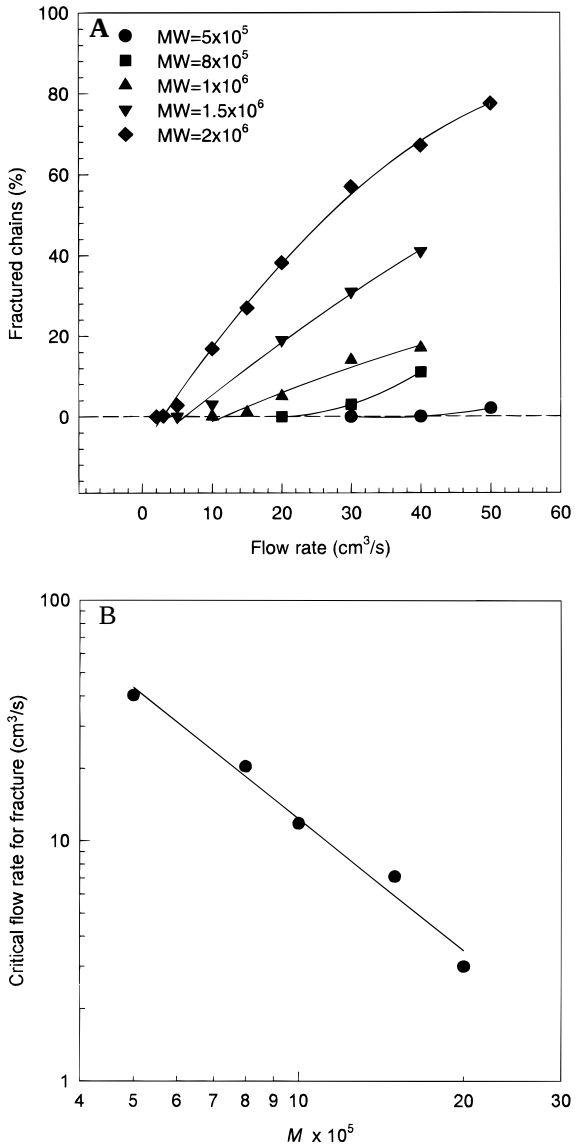

Figure 9. (A) Fracture yield at the capillary orifice vs flow rate for polystyrene with different molecular weights. HI was not included in the simulations. In the simulations ensembles of 100 polymer chains were used at each molecular weight and each flow rate. (B) Log−log plot of relationship between critical flow rate for fracture and molecular weight.

which corresponds to the polymer/solvent system used in our study, the exponent will be −1.0, which agrees well with the result obtained in our study when HI was included (−0.95).

The fact that, in our simulated transient flow, Q_{crit} is proportional to M^{-2} when HI is neglected, while Q_{crit} scales with M^{-1} (roughly) with HI, implies in the limit of very long chains that fracture is hindered by the HI effect. Depending on the value of the scaling exponents, there can be a crossover of the two cases. Indeed, this happens with our results, since the critical flow curves reported in Figures 9B and 10 intersect each other at a M value of 8×10^5. Thus a polystyrene chain with M smaller than that value is easier to break (lower Q_{crit}) due to HI or, conversely, more difficult to degrade if HI were absent. However, the observation and the location of this crossover may not be really significant, due to its probable dependence on modeling and simulation details, and at any rate, the no-HI case does not exist in practice and has essentially theoretical interest.

Figure 11 compares the simulation results for the fracture (percent of total number of chains) with and without HI, monitored at the capillary orifice. We note that when HI is included the fracture yield is lower. Apart from this, the critical flow rate for fracture is observed to be higher in the HI case (about 10 cm^3/s) than in the no-HI case (about 4 cm^3/s). This corresponds well with the arguments used above concerning the reduction in chain extension due to hydrodynamic interaction.

In summary, the main effects from HI are as follows. The flow rate has a larger threshold value, Q_{crit}, when HI is included. However, the dependence of Q_{crit} on the molecular weight is much weaker with HI, with a scaling exponent that is reduced by HI to roughly one-half the no-HI exponent.

In the case of steady elongational flow, one of the conditions claimed to be necessary for chain fracture is that the fluid strain rate must exceed the value $1/\tau_1$, where τ_1 is the primary relaxation time of the chain.[21] In our case, the Rouse relaxation time was equal to 73 μs. When hydrodynamic interaction is taken into consideration, the relaxation time will be lower, and the so-called Zimm relaxation time (including HI in an equilibrium-averaged manner) can be estimated by

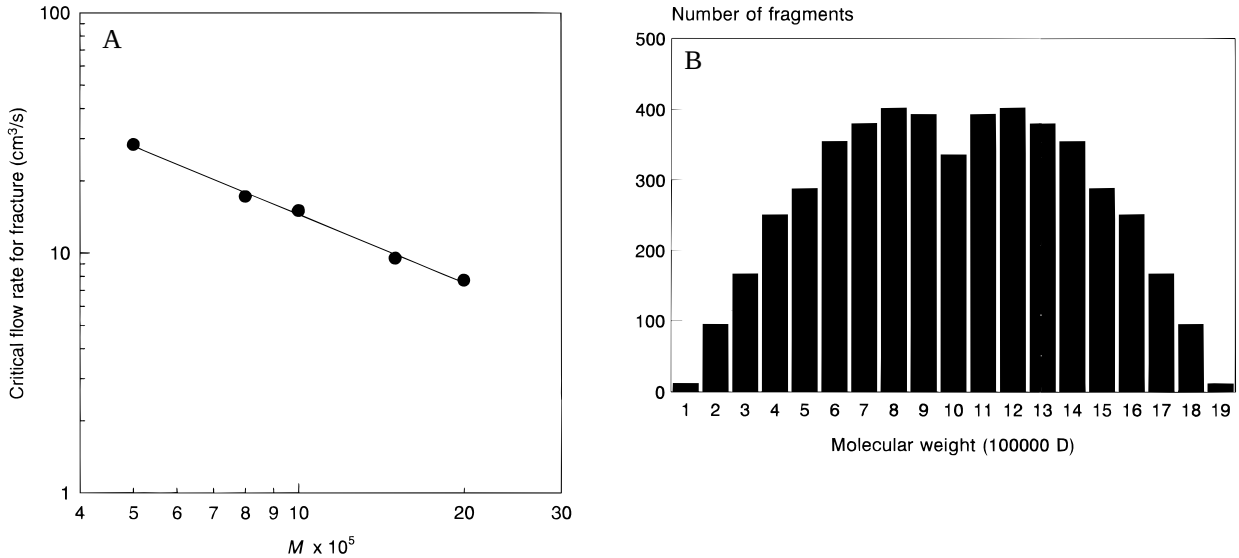

Figure 10. (A) Log−log plot of relationship between critical flow rate for fracture at the orifice and molecular weight with HI included in the simulations. Ensembles of 200 chains were used to obtain the critical flow rate. (B) Distribution of molecular weight of the fracture fragments of polystyrene ($M = 2 \times 10^6$) at the capillary orifice with HI included. Volumetric flow rate (Q) = 25 cm^3/s. For obtaining the molecular weight distribution, the ensemble consisted of 5000 polymer chains.

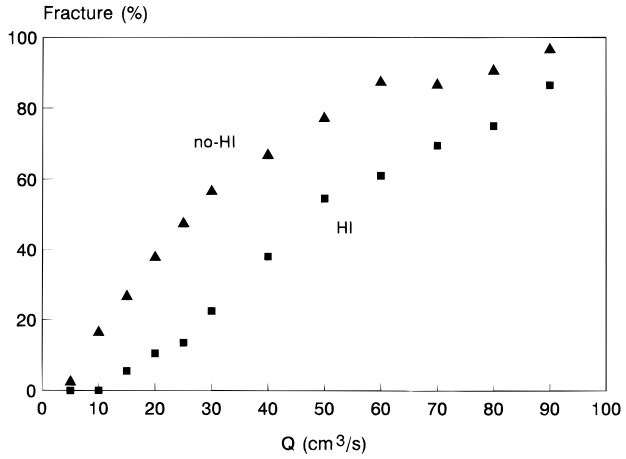

Figure 11. Fracture yield at the capillary orifice vs flow rate for polystyrene with molecular weight equal to 2×10^6. Two cases, with and without HI, are shown. For each flow rate 500 (no-HI) and 200 (HI) chains were used in the simulations.

means of an equation given by Thurston,[26] from which we obtain $\tau_{1,\mathrm{HI}} = 40\ \mu$s. In this case we get $1/\tau_{1,\mathrm{HI}} = 0.25 \times 10^5\ \mathrm{s}^{-1}$. A volumetric flow rate of 10 cm^3/s, which we obtained as the lower limit for fracture in the HI case, corresponds to a maximum value of $\dot{\epsilon}$ equal to ca. $1.4 \times 10^6\ \mathrm{s}^{-1}$ (see Figure 2). This means that the extensional rate necessary for fracture in our setup is considerably higher (ca. with a factor of 50) than the lower limit in steady elongational flow conditions. This is probably due to the fact that in transient extensional flow, the flow is inherently without the persistently extensional character[21] that is connected with chain fracture in the steady flow case.

Although our model of the flow pattern in the simulated device was simplified using clearly defined mathematical borders between the different regions of flow, we believe that we have taken care of the most important aspects regarding how the convergent flow influences the behavior of the polymer chains, thus giving results that are at least qualitatively credible.

Some aspects of our results can be compared to findings in previous works on related problems or to existing knowledge in the field (the following discussions are based on the comments and information kindly supplied by a referee). In the problem simulated in our work, the extensional rate is position-dependent, and therefore, as the macromolecule moves in the flow, it experiences a time-dependent rate. Nonetheless, the overall picture of chain deformation observed in our simulation has some similarities with results from simulations in homogeneous or steady flows. Thus, for the moderate flow rate used in Figures 3−5, the overall dimensions $\langle R^2 \rangle$ and $\langle S^2 \rangle$ increase by a factor of 3, while the spring elongation $\langle q^2 \rangle$ increases by a factor of, at most, 1.3 for the central bond. This indicates that the molecule is deformed by opening the included angles between neighbor springs, so adopting a more prolate conformation, as in the simulations of Wiest et al.[27] Nonetheless, the chain may reach a fully stretched conformation (Figure 6B) as noted by those authors. Also, in all cases we observe that stretching is mainly concentrated at the center of the chain, as noted in other simulations.[28,29]

The springs in the model chain correspond to parts (subchains) in the real polymer molecule. Therefore, our criterion based on a limiting energy required for spring fracture would correspond to a mechanism of global energy accumulation. This may be in the line of a hypothesis of existence of cooperative modes for bond scission,[30] although most mechanochemical degradation studies have been based on a different view, namely, the notion of local stress or strain of individual bonds, like in the TABS model of Odell.[31] Unfortunately, coarse-grained bead-and-spring models cannot describe that notion. It is also noticeable that the molecular weight distribution obtained in our simulation is broader than that found in experiments or from the TABS model. Actually, our distribution resembles the parabolic distribution of stress along the molecular chain, theoretically deduced from slender body hydrodynamics in elongational flow.[32]

Concluding Remarks

Due to the incomplete understanding of the behavior of polymer chains when they are exposed to extensional flow of transient type, we have in this study used a numerical simulation technique to study conformation and fracture of a model of polystyrene as an alternative to experimental and analytical treatments. The simulated device consisted of a tube from which the solution of polystyrene in cyclohexane is forced to flow into a capillary. We observed large chain extensions and chain fracture in the capillary orifice, with a fracture yield strongly dependent on flow rate. The relation between critical flow rate for fracture and molecular weight was found to depend strongly on whether the hydrodynamic interaction effect was taken into consideration or not. Hydrodynamic interaction also influenced the fracture yield, giving a reduced fracture when this effect was included. These results indicate that hydrodynamic interaction should not be disregarded in analytical or numerical treatments of polymer fracture in extensional flow.

Acknowledgment. We are grateful to an anonymous referee for comments and references that improved the discussion of our results. We acknowledge support from grants PB93-1132 (DGCYT-MEC) and PIB94-07 (DGUI-CARM). K.D.K. acknowledges Grant ERBCHBICT 940974 from the Commission of the European Communities.

References and Notes

(1) Odell, J. A.; Keller, A.; Miles, M. J. *Polym. Commun.* **1982**, *24*, 7.
(2) Müller, A. J.; Odell, J. A.; Keller, A. *J. Non-Newt. Fluid Mech.* **1988**, *30*, 99.
(3) Odell, J. A.; Keller, A.; Müller, A. *J. Colloid Polym. Sci.* **1992**, *270*, 307.
(4) Nguyen, T. Q.; Kausch, H.-H. *J. Non-Newt. Fluid Mech.* **1988**, *30*, 125.
(5) Nguyen, T. Q.; Kausch, H.-H. *Macromolecules* **1990**, *23*, 5137.
(6) Fuller, G. G.; Leal, L. G. *Rheol. Acta* **1980**, *19*, 580.
(7) Fuller, G. G.; Cathey, C. A.; Hubbard, B.; Zebrowski, B. E. *J. Rheol.* **1987**, *31*, 23.
(8) Reese, H. R.; Zimm, B. H. *J. Chem. Phys.* **1990**, *92*, 2650.
(9) López Cascales, J. J.; García de la Torre, J. *J. Chem. Phys.* **1991**, *95*, 9384.
(10) López Cascales, J. J.; García de la Torre, J. *J. Chem. Phys.* **1992**, *97*, 4549.
(11) Knudsen, K. D.; Hernández Cifre, J. G.; López Cascales, J. J.; García de la Torre, J. *Macromolecules* **1995**, *28*, 4660.
(12) Bird, R. B.; Curtiss, C. F.; Armstrong, R. C.; Hassager, O. *Dynamics of Polymeric Liquids. Volume 2. Kinetic Theory*; John Wiley & Sons: New York, 1987.
(13) Schmidt, M.; Burchard, W. *Macromolecules* **1981**, *14*, 210.
(14) Huber, K.; Bantle, S.; Lutz, P.; Burchard, W. *Macromolecules* **1985**, *18*, 1461.
(15) Ermak, D. L.; McCammon, J. A. *J. Chem. Phys.* **1978**, *69*, 1352.
(16) Iniesta, A.; García de la Torre, J. *J. Chem. Phys.* **1990**, *92*, 2015.

(17) Yamakawa, H. *J. Chem. Phys.* **1970**, *53*, 436.
(18) Chauveteau, G.; Moan, M.; Magueur, A. *J. Non-Newt. Fluid Mech.* **1984**, *16*, 315.
(19) Liu, T. W. *J. Chem. Phys.* **1989**, *90*, 5826.
(20) Rabin, Y. *J. Chem. Phys.* **1988**, *88*, 4014.
(21) Keller, A.; Odell, J. A. *Colloid Polym. Sci.* **1985**, *263*, 181.
(22) Odell, J. A.; Keller, A. *J. Polym. Sci., Polym. Phys. Ed.* **1986**, *24*, 1889.
(23) López Cascales, J. J.; López Martínez, M. C. *Anal. Química* **1991**, *87*, 816.
(24) Rabin, Y. *J. Chem. Phys.* **1987**, *86*, 5215.
(25) Rabin, Y. *J. Non-Newt. Fluid Mech.* **1988**, *30*, 119.
(26) Thurston, G. B. *Polymer* **1974**, *15*, 569.
(27) Wiest, J. M.; Wedgewood, L. E.; Bird, R. B. *J. Chem. Phys.* **1989**, *90*, 587.
(28) Larson, R. G.; Magda, J. J. *Macromolecules* **1989**, *22*, 3004.
(29) Lopez Cascales, J. J.; Navarro, S.; Garcia de la Torre, J. *Macromolecules* **1992**, *25*, 3574.
(30) Tomashevskii. *Sov. Phys.-Solid State* **1971**, *12*, 2588.
(31) Odell, J. A.; Keller, A.; Rabin,Y. *J. Chem. Phys.* **1988**, *88*, 4022.
(32) Frenkel, Y. *Acta Physicochim. USSR* **1944**, *19*, 51.

MA9513980